Interpretation of the diffuse scattering in Pb-based relaxor ferroelectrics in terms of three-dimensional nanodomains of the ⟨110⟩-directed relative interdomain atomic shifts

Marek Paściak, Marek Wołcyrz, and Adam Pietraszko
Institute of Low Temperature and Structure Research, Polish Academy of Sciences, P.O. Box 1410, Wrocław 2, Poland
(Received 20 December 2006; revised manuscript received 14 March 2007; published 26 July 2007)

Polar nanoregions in relaxor ferroelectrics were modeled by the Monte Carlo method. To account for correlations between atomic shifts, Potts-like models were applied with a random field used to mimic the chemical disorder impact on the polar ordering. The diffuse scattering effects for generated structures were calculated and compared with the neutron and x-ray experimental data known from the literature. An alternative explanation of diffraction effects contrary to the polar "pancakes" concept reported in several recent papers is given. Generated three-dimensional polar domains with the walls parallel to {110}-type crystallographic planes result in one-dimensional diffuse scattering rods fully compatible with the experimental results. Moreover, special extinction conditions for diffuse lines clearly indicate that the relative shifts of the atoms in the neighboring domains have to be parallel to ⟨110⟩-type directions. This can be achieved by various combinations of atomic shifts. Therefore, it is impossible to elucidate their actual directions based only on the analysis of the diffuse scattering effects. We show that the intensities of diffuse scattering are sensitive to the relative magnitudes of the atomic displacements and can be used as a starting point for their determination.

DOI: 10.1103/PhysRevB.76.014117 PACS number(s): 77.80.−e, 77.84.Dy, 61.43.Bn

I. INTRODUCTION

Relaxor ferroelectrics (RFEs) are technologically important materials with extraordinary dielectric and electromechanical properties and possible applications as transducers and actuators. Chemically disordered Pb-based RFEs [Pb-RFEs, e.g., $Pb(Mg_{1/3}Nb_{2/3})O_3$ (PMN), $Pb(Zn_{1/3}Nb_{2/3})O_3$ (PZN), $Pb(Sc_{1/2}Nb_{1/2})O_3$ (PSN), and $Pb(Sc_{1/2}Ta_{1/2})O_3$ (PST)] manifest typical relaxor properties (high value of permittivity, its broad-diffuse dependence on temperature and strong dependence on frequency, weak remnant polarization).[1,2] Chemical ordering, as well as doping (e.g., with Ti), can suppress relaxor behavior in these compounds.

Pb-RFEs belong to the family of $Pb(B',B'')O_3$-type perovskite compounds. Their crystal structures were extensively studied by various techniques in both nonpolar paraelectric and polar ferroelectric phases.[3–17] According to the results of the conventional x-ray and neutron structure analyses performed on single crystals and powders, Pb-RFEs crystallize in a set of unit cells closely related to the basic perovskite cubic cell with $a \approx 4$ Å. However, despite all of the performed studies, certain controversies remain over the crystal structures of Pb-RFEs. The difficulties in their adequate description and determination result from the complex real structure. As revealed by many electron microscopic studies,[5–7,10,11,13,18–23] the real structure of Pb-RFEs in their relaxor state consists of two types of ordered nanodomains, chemical and polar, occurring in the disordered matrix. The papers obviously show the three-dimensional character of the nanodomains. It is this fact which is not always taken into account when interpreting, e.g., diffuse scattering effects produced by RFEs.

The problems concerning the determination of the real crystal structure of RFEs cannot be overcome with conventional structure analysis treating crystal globally and giving the average structure. A better tool for local structure analysis is the interpretation of diffuse scattering, appearing in the reciprocal space aside from Bragg reflections and related to additional correlations taking place in the crystal. There is an opinion[24,25] that for the RFE in its relaxor state, the main contribution to diffuse scattering is coming from static disorder, namely, from polar domains, instead of thermally activated inelastic scattering. Thus, the careful analysis of the x-ray, electron, or neutron diffuse scattering can supply essential information on the local structure of the materials: short-range order and correlation of the atomic displacements or occupations. The numerous examples of such analysis for a wide spectrum of materials are described in the fundamental book of Welberry.[26] In recent years, many papers appeared presenting and interpreting the diffuse scattering effects observed with neutrons or x rays on Pb-RFEs.[24,25,27–35]

The unique properties of RFEs are usually considered to be related to polar nanoregions (PNRs) and these, in turn, are thought to be the result of chemical disorder. Therefore, there exists two types of mutually related disorders in the relaxor structure: the atomic displacements and occupational disorder of B' and B'' atoms. When modeling relaxor properties, one has to cover this duality. According to Burton *et al.*,[36] the elucidation of the relationship between chemical short-range order and polar nanodomains and their respective length scales is a long-standing and central problem in the RFE studies.

There is a concept of random field in ferroelectrics given by Halperin and Varma.[37] They derived it from the works on ferromagnets and found that random field coming from an occupational disorder could limit long-range polar order and smear the ferroelectric phase transition. This concept was widely investigated in the subsequent works. Qian and Bursill[38] used Monte Carlo (MC) simulation of random field Potts model to investigate polar domain formation and mutual relation between chemical and ferroelectric orderings. Fisch[39] studied the four-state clock model (also known as a vector Potts model) with random field to evaluate correla-

tions between electric dipoles in RFE. Recently, Burton *et al.*[36,40] and Tinte *et al.*[41] performed molecular dynamics simulations on a first-principles effective Hamiltonian model.[42] They introduced the random field term into the model with values derived from the calculations based on electrostatic point-charge model.

The aim of the present paper is the interpretation and explanation of the origin of the diffuse scattering effects observed in Pb-RFEs in terms of three-dimensional nanodomains of the ⟨110⟩-directed relative interdomain atomic shifts. Starting from simple models—Ising model and vector Potts model with random field and then extending it—we simulate by the Monte Carlo method the nanodomain structure of RFEs containing both chemical and polar domains. The verification of the models and their parameters applied for simulations is the comparison of the diffraction effects obtained for the modeled crystal with the experimental data collected with neutrons and x rays and presented in the literature. The results fitting the experimental data allow us to understand better the structure of PNRs.

It should be emphasized that we are not aiming to model RFEs in their full complexity. Issues such as the character of phase transformation and its dependence on chemical disorder are out of the scope of this paper. Our purposes are simpler—the modeling is basically the tool for generating various crystal configurations (or, in other words, a method of imposing correlations into the structure), which can then be verified with experimental diffraction data. Following Welberry *et al.*,[31] we can state that the emphasis is to say what is happening (what is the structure of correlations in crystal) rather then why it is happening.

II. DIFFUSE SCATTERING DATA

From many papers presenting the results of diffuse scattering in Pb-RFEs mentioned in the Introduction, we have chosen three data sets of the best quality, i.e., for PMN, registered with x rays (Stock *et al.*[35]), for PZN, registered with neutrons (Welberry *et al.*[31]), and for PZN, registered with x rays (Xu *et al.*[25]). We also take into account our data obtained for PST with x rays.[43,44] We have treated all of these data as a point of reference for our modeling. They are consistent to a large extent and reveal common features presented in Fig. 1, which is a graphical reconstruction combining results reported for all three compounds.

The most characteristic feature of the diffuse scattering patterns presented in Fig. 1 as $(hk0)$ and $(hk1)$ sections of the reciprocal space is the existence of diffuse lines running through the Bragg spots perpendicularly to the set of ⟨110⟩ directions in the reciprocal space [note that $\langle uvw\rangle$ stands for a set of all symmetrically equivalent lattice directions $[uvw]$ both in direct and in reciprocal space; similarly, $\{hkl\}$ stands for a set of all symmetrically equivalent net planes (hkl)]. More detailed, three-dimensional scans of the reciprocal space[25,34] showed that the lines are in fact one-dimensional rods forming characteristic butterflies and ellipsoids around Bragg spots. A second feature of the diffuse patterns is the lack of [110] and $[\bar{1}10]$-directed diffuse lines passing through the centers of the pictures and the increasing intensity of diffuse rods with the distance from the origin of the reciprocal space. This feature can be observed on both $(hk0)$ and (hkl) layers and in fact all {110}-type planes are subject to extinction. A third, more subtle feature observed by Welberry *et al.*[31] is a kind of extinction limiting the possibility of diffuse scattering lines passing certain Bragg reflections in the (hkl) layer: diffuse rods appear when $h+k=$odd; for $h+k=$even, they seem to be extinct or at least distinctly weaker.

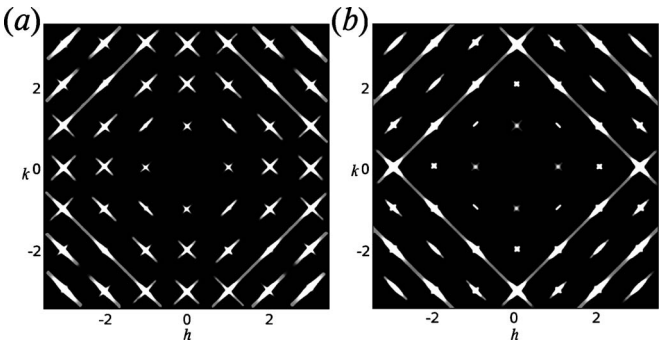

FIG. 1. The sections of the reciprocal space for Pb-RFEs reconstructed from the data given in Refs. 25 and 31 (for PZN), 35 (PMN), and 43 and 44 (PST): (a) $(hk0)$ layer; (b) $(hk1)$ layer (Miller indices given in ~4 Å matrix cell).

III. MODELING AND RESULTS

By building structural models giving characteristic diffuse scattering, we follow the concepts presented in the Introduction, i.e., investigate simple spinlike models and take into account chemical disorder applying quenched random field to them. Since we put the main effort here into the explanation of the diffraction effects, which are observed both in neutron and x-ray experiments, the assumption that correlations between displacements of cations play the most important role seems to be reasonable. Thus, the investigated systems have the CsCl structure—Pb and B'/B'' atoms occupy sites on simple cubic sublattices; oxygen atoms are not taken into account during the first stage of modeling. Therefore, as a result, we obtain the structure of cationic displacements. Such a structure is the subject for further modifications in the second stage of modeling by the optimization of the magnitudes of the atomic shifts of both cations and oxygen. As will be discussed later, such modification cannot change the general shape of diffuse scattering although it affects its intensity.

A. Chemical domains

We deal with compounds of different stoichiometries at B'/B'' sites—1:1 (PST, PSN) and 1:2 (PMN, PZN). In some of 1:1 relaxors (PST), chemical long-range order (LRO) appears—B' and B'' cations tend to alternate, forming large chemical domains, whereas the others (PSN) and 1:2 compounds (PMN, PZN) have been only synthesized with some short-range order (SRO), i.e., with small statistically ordered

areas in a disordered matrix. In the case of 1:2 compounds, this statistical chemical order means that one B-site sublattice is occupied by the B'' atoms and the second is randomly occupied by both B'' and B' atoms in the 1:2 ratio (random-site model). Clearly, two different strategies are needed to accurately reproduce chemical LRO and SRO. In the case of the first one, the distribution of B' and B'' atoms were generated by the MC method using the next nearest neighbors Ising (NNNI) model[31,45] with the help of a spin-exchange Metropolis algorithm.[46]

The MC simulations of chemical domains (as all other simulations performed in this paper) were done on a finite three-dimensional network of 50^3 unit cells of matrix phase ($Pm\bar{3}m$ space group, a=4.08 Å) with periodic boundary conditions. The simulation for the 1:1 structure with the nearest neighbor and the next nearest neighbor coupling constants $J_{nn}=0.1kT$ and $J_{nnn}=-0.1kT$, respectively, and 10 000 MC steps resulted in a chemical structure for which the ratio of sites having atoms of a different type as a nearest neighbor to the total number of B sites was ~0.725.

For 1:2 structures, the NNNI model can lead to the phase separation into ordered B'/B'' domains and homogeneous areas consisting only of B'' atoms; such a situation was proven to be unrealistic.[47] To properly account for SRO, we have applied a similar strategy as Burton *et al.*,[40] i.e., we introduced 20 statistically ordered domains with the size of 10^3 unit cells (~4 nm) in a completely disordered matrix.

In all performed simulations, random field values are nonzero only on the Pb sites, and they are derived from charge imbalance in the environment of lead in the same way as done by Qian and Bursill.[38] Thus, the random field vector $\mathbf{h}_i$ for a given site i is simply a vector sum of contributions from four pairs of B'/B'' atoms connected via diagonals:

$$\mathbf{h}_i = \mathbf{a}_1 + \mathbf{a}_2 + \mathbf{a}_3 + \mathbf{a}_4, \tag{1}$$

where $|\mathbf{a}_i|=0$ for the same atoms, $|\mathbf{a}_i|=1$ for different atoms on the diagonal i, and the sense of $\mathbf{a}_i$ is toward the cation of the lower charge of the B'/B'' pair.

In Fig. 2, two-dimensional sections of 1:1 (with LRO) and 1:2 (with SRO) chemical structures used in subsequent calculations with respective random field configurations are shown. It is seen that for 1:1 structures [Fig. 2(a)], the shape of the random field is strictly correlated with the distribution of very visible chemical domains, whereas for 1:2 structure [Fig. 2(b)] nonzero random field is ubiquitous.

According to the expectations, the chemical disorder has no practical impact on the diffuse scattering observed. The only visible effects are the increasing and sharpening of the superstructure reflections of the $h+1/2$, $k+1/2$, $l+1/2$ type vs increasing degree of chemical order.

B. Polar domains

There is a controversy about the direction of atomic displacements within polar domains. Since a cubic to rhombohedral phase transition is observed in most RFEs, ⟨111⟩-type directions seemed to be the natural guess.[21,24] However, in recent works,[25,31,34,48] a shape of diffuse scattering led authors to consider PNRs as the {110}-oriented planes (or "pancakes") with polarization (i.e., atomic displacements) along the plane. Also, ⟨100⟩ directions of Pb displacements were derived from pair-density function analysis for PST.[16] Moreover, for PST, as well as for PMN and PZN, tetragonal distortion was reported for different magnitudes of doping with Ti.[49–51] In order to test these possibilities in our modeling, we restrict the atomic shifts to adopt one of the above mentioned sets of directions. Thus, we test 6-, 8-, and 12-state models for ⟨100⟩, ⟨111⟩, and ⟨110⟩ sets of directions, respectively.

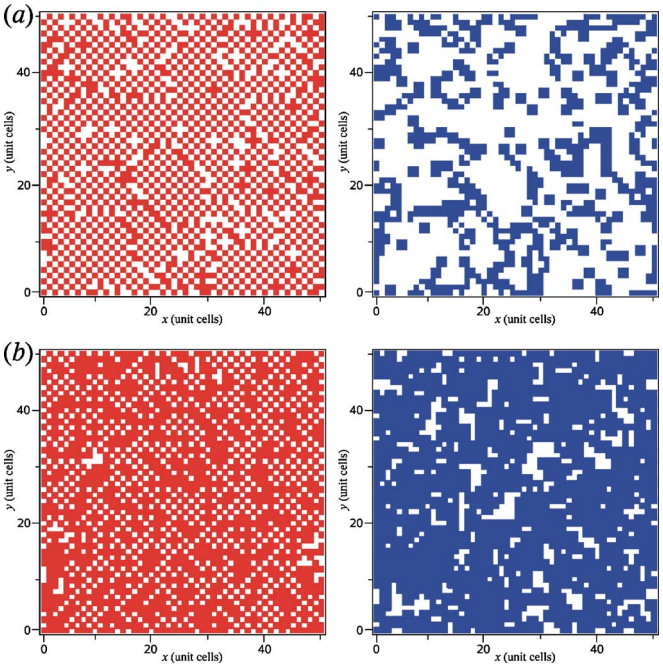

FIG. 2. (Color online) Chemical domain structures (left) and respective random field maps (right) generated for (a) 1:1 stoichiometry with LRO and (b) 1:2 stoichiometry with SRO. In structure representation pictures, white and red squares represent B' and B'' atoms. On random field maps: white squares are the zero field and blue squares are the nonzero field. Sections are by the xy plane of the crystal.

MC procedures for energy minimization for all models of polar domains were based on the Metropolis algorithm.[46] In order to equilibrate the system more efficiently, a simulated annealing scheme was applied. Each simulation was started in a high temperature range (~$3J$) and kT was slowly decreased ($0.25J/1000$ MC steps). Simulation at the final temperature lasted until there was no change in the energy of the system (usually 5000 MC steps). Simulated crystals with an obtained domain structure were objects for which diffraction effects were calculated by means of the DISCUS program. The KUPLOT routine, together with DISCUS, forming a part of the DIFFUSE package,[52] was a tool for the graphical presentation of diffraction results. The program DISCUS calculates the Fourier transform according to the standard formula for kinematic scattering:

$$F(\mathbf{h}) = \sum_{i=1}^{N} f_i(\mathbf{h}) \exp(2\pi i \mathbf{h}\cdot\mathbf{r}_i) \exp(-B|\mathbf{h}|^2/4). \tag{2}$$

The finite-size effect was avoided by the application of periodic boundary conditions: $\Delta h = 1/\Delta x$, where Δh is the grid

size of the calculated reciprocal layer and Δx is the corresponding dimension of the modeled crystal.

We present our results in a stepwise manner: firstly, the application of the vector Potts model is presented; then, after the comparison of calculated diffuse scattering patterns with experimental results and their verification, effects of simulation for two model extensions are shown.

1. Potts model

In order to simulate the polar domain structure, one has to consider different directions of atomic displacements, and therefore needs a many-state model. Qian and Bursill[38] chose the simplest standard Potts model with the Hamiltonian of the form

$$H^{SP} = -J\sum_{\langle i,j\rangle} \delta(\boldsymbol{\sigma}_i, \boldsymbol{\sigma}_j) - \sum_i \boldsymbol{\sigma}_i \cdot \mathbf{h}_i, \tag{3}$$

where the first sum is over nearest neighbors, J is the coupling constant, $\boldsymbol{\sigma}_i$, $\boldsymbol{\sigma}_j$ are the Potts variables (in our case vectors of displacement), and $\mathbf{h}_i$ are the random field values.

We took into account the simple generalization of the vector model proposed by Potts.[53] He considered a system of spins spaced in one of the n directions equiangularly arranged in the same plane. For three dimensions and with the addition of the random field term, we can formulate the Hamiltonian of the random field vector Potts (RFVP) model as follows:

$$H^{RFVP} = -J\sum_{\langle i,j\rangle} \boldsymbol{\sigma}_i \cdot \boldsymbol{\sigma}_j - D\sum_i \boldsymbol{\sigma}_i \cdot \mathbf{h}_i, \tag{4}$$

where $\langle i,j\rangle$ stands for nearest neighbors, $\boldsymbol{\sigma}_i$, $\boldsymbol{\sigma}_j$ are vectors indicating displacements on sites i and j, $\mathbf{h}_i$ is the random field term, and D stands for the random field coupling constant.

The basic achievement of the RFVP model is the generation of polar nanodomains, which results in diffuse scattering partially compatible with the experimental patterns. The results of the simulation are presented in Fig. 3, where the structure of Pb atom displacements (in this case $\boldsymbol{\sigma}_i \| \langle 111\rangle$), as well as ($hk0$) and ($hk1$) sections of the reciprocal space, is shown. It is obvious that the results obtained are independent of the set of directions chosen in the simulation—it results from the form of the Hamiltonian. It is seen that diffuse scattering forms characteristic diagonal lines in both ($hk0$) and ($hk1$) layers, but there are no visible extinctions of the [110] and [$\bar{1}$10]-directed central lines, as well as $h+k$=even extinctions in the ($hk1$) layer. The explanation of such diffraction effects is as follows. It is well known that diffuse scattering in the shape of streaks or rods is always connected with some planar disorder. Planes, on which atoms are arranged regularly or at least are correlated, should be normal to the diffuse scattering rods.[54] In the case of our simulations, such planar objects are formed by domain walls. Since the domains have different directions of displacement, the obtained structures can be considered to contain stacking faults, which are in fact a kind of planar disorder and cause one-dimensional diffuse scattering effects. Welberry *et al.*[31] also obtained diffuse streaks; but in their case, the reason for the shape of the scattering is in the polar layers, which seems to be in contradiction with microscopical evidence of three-dimensional PNRs. In our case, the simulation leads to three-dimensional PNRs the boundaries of which tend to be normal to ⟨110⟩ directions [cf. Fig. 3(a)] because such a configuration minimizes the energy of domain boundaries. However, the nature of domain boundaries, or more precisely, the correlation between atomic shifts of the neighboring domains is of such a kind that more subtle details of the diffuse scattering do not appear: neither line extinctions nor their intensity variation with the distance from the origin is present in the generated patterns.

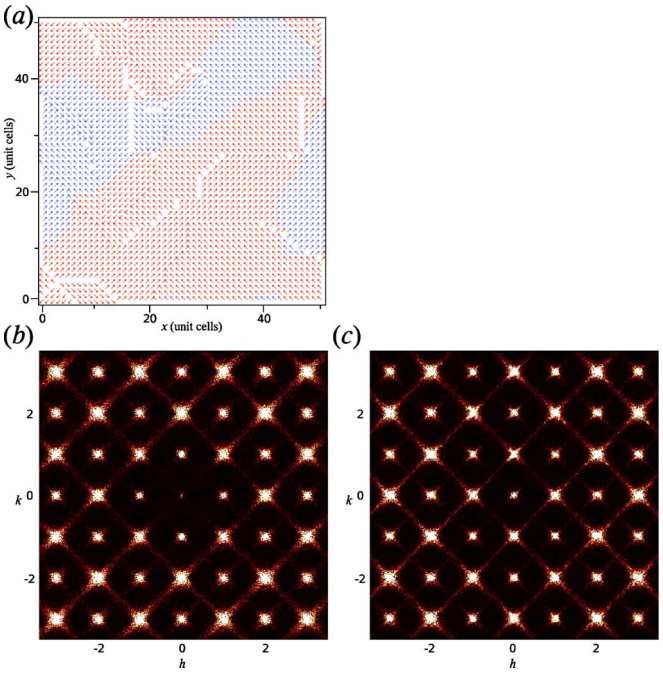

FIG. 3. (Color online) (a) Polar domain structure and [(b) and (c)] diffraction effects obtained using vector Potts model with random field for ⟨111⟩ directions of the atomic shifts. 1:1 chemical structure with LRO, $kT=1/4\ J$, $D=J$. Arrows represent atomic shifts along ⟨111⟩; colors depict their sense: red is up and blue is down the plane of the picture. Sections are by the xy plane of the crystal and (b) ($hk0$) and (c) ($hk1$) layers of the reciprocal space.

2. Model extensions

It is well known that in the case of displacement disorder, diffuse intensity varies as $(\mathbf{q}\cdot\Delta\boldsymbol{\sigma})^2$, where $\mathbf{q}$ is the reciprocal space vector and $\Delta\boldsymbol{\sigma}$ is the relative displacement of atoms.[55] Thus, extinctions indicate that every structural feature causing diffuse scattering must include displacements giving $\mathbf{q}\cdot\Delta\boldsymbol{\sigma}=0$. As we discussed before, in our case, {110}-type planes are subject to extinction. Therefore, $\Delta\boldsymbol{\sigma}$ must adopt one of the ⟨110⟩-type directions. The way to combine this fact with the concept of {110}-type domain walls is to consider possible relative displacements of the atoms in the two neighboring domains. It is straightforward to see that within every mentioned set of atomic shifts (⟨111⟩, ⟨110⟩, and ⟨100⟩), there are combinations of displacements, which can lead to relative ⟨110⟩-type shifts. Examples of such combi-

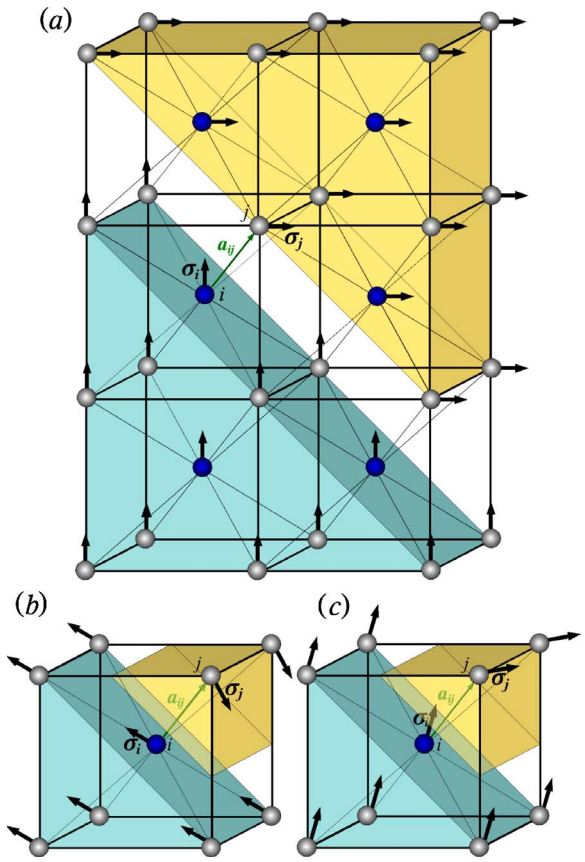

FIG. 4. (Color online) Examples of the specific atomic shifts $(\boldsymbol{\sigma}_i, \boldsymbol{\sigma}_j)$ leading to the ⟨110⟩-directed relative interdomain atomic shifts for three different directions of displacements. Two polar domains are depicted by different colors. (a) $\boldsymbol{\sigma}_i \| [001]$, $\boldsymbol{\sigma}_j \| [010]$, $\boldsymbol{\sigma}_j - \boldsymbol{\sigma}_i \| [01\bar{1}]$; (b) $\boldsymbol{\sigma}_i \| [\bar{1}01]$, $\boldsymbol{\sigma}_j \| [\bar{1}10]$, $\boldsymbol{\sigma}_j - \boldsymbol{\sigma}_i \| [01\bar{1}]$; (c) $\boldsymbol{\sigma}_i \| [1\bar{1}1]$, $\boldsymbol{\sigma}_j \| [11\bar{1}]$, $\boldsymbol{\sigma}_j - \boldsymbol{\sigma}_i \| [01\bar{1}]$.

nations are shown in Fig. 4 for three different sets of atomic shift directions. Thus, in order to obtain the demanded shape of diffuse scattering, it is necessary to modify the RFVP model in such a way that the new model leads to the formation of polar domains with the required relationship between their atomic shifts. Below, we test two types of such Hamiltonians.

(a) Model for ⟨100⟩ and ⟨110⟩ atomic shifts. To try to find a better model, we should first think of what in the RFVP model and other spinlike models can be neglected. The issue one can immediately devise is the fact of the insensitivity of the model to the positions of atoms. The energy contribution of the configuration containing $\boldsymbol{\sigma}_i$ and $\boldsymbol{\sigma}_j$ is always $J\boldsymbol{\sigma}_i \cdot \boldsymbol{\sigma}_j$ independently of the relative positions of the i and j sites. If we take into account, for example, $\boldsymbol{\sigma}_i \| [100]$ and neighboring j site for which interatomic vector $\mathbf{d}_{ij} \| [111]$, the energy contribution is the same for $\boldsymbol{\sigma}_j \| [0\bar{1}0]$, $[00\bar{1}]$, $[010]$, and $[001]$, whereas for the first two directions, atoms are approaching each other, and for the last two, the interatomic distance remains almost unaltered. The way to differentiate these two situations is to change the model so that it prefers configurations which preserve interatomic distances. The difference between squares of the interatomic distances calculated before $(\mathbf{a}_{ij})$ and after $(\mathbf{b}_{ij})$ shifting the atoms is

$$\mathbf{b}_{ij}^2 - \mathbf{a}_{ij}^2 = (\boldsymbol{\sigma}_j - \boldsymbol{\sigma}_i) \cdot (2\mathbf{d}_{ij} + \boldsymbol{\sigma}_j - \boldsymbol{\sigma}_i), \tag{5}$$

where $\mathbf{d}_{ij}$ is the vector linking i and j sites. Therefore, we can write the Hamiltonian of our "distance preserving" model in the form

$$H = -J \sum_{\langle i,j \rangle} \exp\{-C[(\boldsymbol{\sigma}_j - \boldsymbol{\sigma}_i) \cdot (2\mathbf{d}_{ij} + \boldsymbol{\sigma}_j - \boldsymbol{\sigma}_i)]^2\} - D \sum_i \boldsymbol{\sigma}_i \cdot \mathbf{h}_i, \tag{6}$$

where $\boldsymbol{\sigma}_i$ is the displacement vector for the atom at site i, $\mathbf{d}_{ij}$ the vector linking i and j sites, J and D the coupling constants, C the constant controlling the energy distance between different displacement configurations, $\langle i,j \rangle$ the nearest neighbors, and $\mathbf{h}_i$ the random field vector. During the simulations, we make an assumption that $|\boldsymbol{\sigma}|/|\mathbf{d}| = 0.1$, but the magnitudes of the atomic shifts in the final structures are optimized, being for most of the results 5% and 2.5% of cubic lattice parameter for Pb and B'/B'' atoms, respectively.

If we do not take into account the random field, the obvious ground state of the model is the system with fully aligned vectors of displacements. Next, the model favors such configurations of the relative shifts of neighboring atoms $(\Delta\boldsymbol{\sigma}_{ij} = \boldsymbol{\sigma}_j - \boldsymbol{\sigma}_i)$, which are nearly perpendicular to the interatomic distance vector $\mathbf{d}_{ij}$ (long $2\mathbf{d}_{ij}$ vector is slightly modified by a small $\Delta\boldsymbol{\sigma}_{ij}$ term). Because $\mathbf{d}_{ij}$ are along ⟨111⟩ directions, $\Delta\boldsymbol{\sigma}_{ij}$, as perpendicular to it, is one of the ⟨110⟩ sets. Thus, our extended model, apart from being more realistic than the RFVP model, leads to the relative displacements which satisfy the conditions coming from the extinctions of diffuse scattering.

(b) Model for ⟨111⟩ atomic shifts. As already mentioned, the combination of displacements within the ⟨111⟩ set of directions can lead to the relevant relative shifts on the domain walls. However, a distance preserving model cannot be applied, simply because combinations providing ⟨110⟩ relative shifts change the distances between atoms more than the others. In order to produce the domain structure, another more complex model has been applied:

$$H = -J \sum_{\langle i,j \rangle} f(\mathbf{d}_{ij}, \boldsymbol{\sigma}_i, \boldsymbol{\sigma}_j) - D \sum_i \boldsymbol{\sigma}_i \cdot \mathbf{h}_i, \tag{7}$$

where

$$f(\mathbf{d}_{ij}, \boldsymbol{\sigma}_i, \boldsymbol{\sigma}_j) = \begin{cases} 1, & \boldsymbol{\sigma}_j = \boldsymbol{\sigma}_i \\ \dfrac{3}{4}, & (\boldsymbol{\sigma}_j - \boldsymbol{\sigma}_i) \| \langle 110 \rangle \wedge (\boldsymbol{\sigma}_j - \boldsymbol{\sigma}_i) \perp \mathbf{d}_{ij} \\ -1 & \text{otherwise}. \end{cases} \tag{8}$$

Due to the first value of f (for parallel shifts of neighboring atoms), the system prefers domain formation. The second value is responsible for the relevant combination of displacements for neighboring domains. Two conditions have to be fulfilled: the first one assures that the relative interdomain atomic shift is parallel to the ⟨110⟩-type vector; the second one assures that only sites which do not lie on the plane

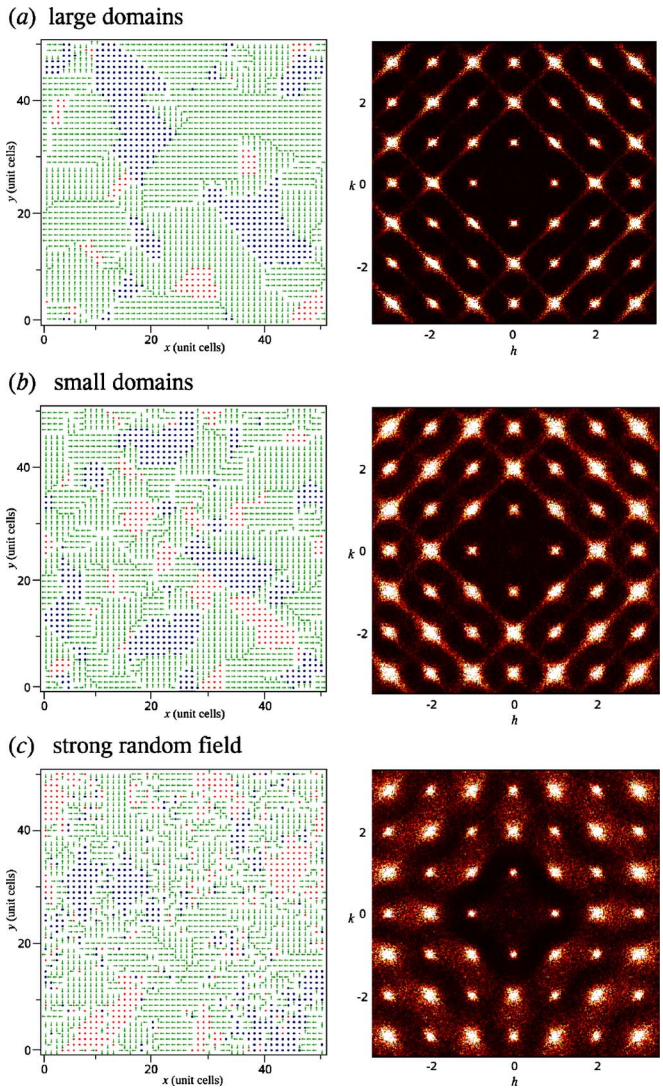

FIG. 5. (Color online) Polar domain structure and diffraction effects obtained for the extended model as a function of parameters. 1:1 chemical structure with LRO, (a) $kT=1.2\,J$, $D=J$, (b) $kT=0.1\,J$, $D=J$, and (c) $kT=0.5\,J$, $D=5J$. Arrows represent different directions of atomic shifts along ⟨100⟩; colors depict their sense: red is up, blue is down, and green is in the plane of the picture. Sections are by the xy plane of the crystal and ($hk0$) layer of the reciprocal space.

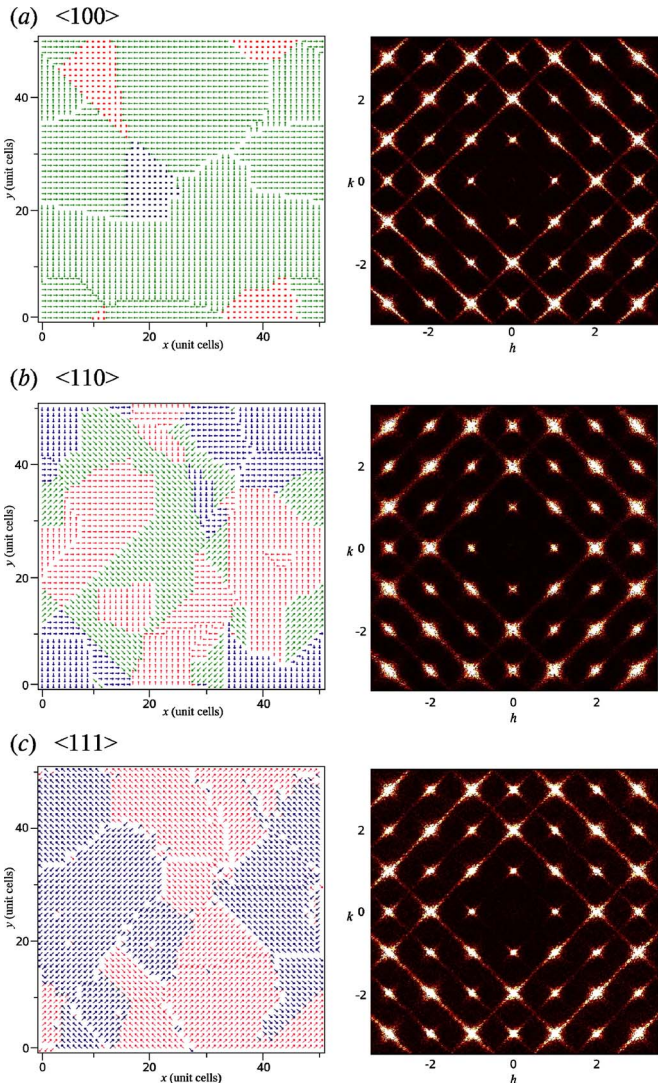

FIG. 6. (Color online) Polar domain structure and diffraction effects obtained for the extended models as a function of direction of the atomic displacements. 1:1 chemical structure with LRO, $kT=1/2\,J$, $D=J$; (a) ⟨111⟩, (b) ⟨110⟩, (c) ⟨001⟩. Arrows represent different directions of the atomic shifts, colors depict their sense: red is up; blue is down, and green is in the plane of the picture. Sections are by the xy plane of the crystal and ($hk0$) layer of the reciprocal space.

spanned by $\boldsymbol{\sigma}_i$ and $\boldsymbol{\sigma}_j$ are taken into account, so that the domain wall can be oriented parallel to such a plane. Relative displacements demanded here do not result from more general assumptions like in the case of the distance preserving model. Therefore, the model for the ⟨111⟩ set of directions seems to be more artificial. However, in the context of papers[56,57] where the concept of mixed ferroelectric and antiferroelectric orderings in relaxors is investigated, one cannot exclude the situation where neighboring domains are almost in antiphase.

(c) Results of the modeling. As already stated, the main use of our models was the generation of the "crystals" consisting of PNRs manifesting required interdomain correlations and producing diffuse scattering patterns known from neutron and x-ray experiments. In order to obtain such results, it is necessary to fit the model parameters. Therefore, the knowledge of the "model behavior" is the first step on this way.

Both extended models lead to the structures with relevant domain walls and relative shifts between neighboring domains, which give rise to the diffuse scattering streaks and appropriate extinctions. Model parameters kT, D, and J can change the domain size and distribution but characteristic interdomain relations are preserved. However, the magnitudes of the atomic shifts influence the intensity relations between diffuse scattering lines.

The influence of the values of parameters used in the simulation on the polar domains and, consequently, on dif-

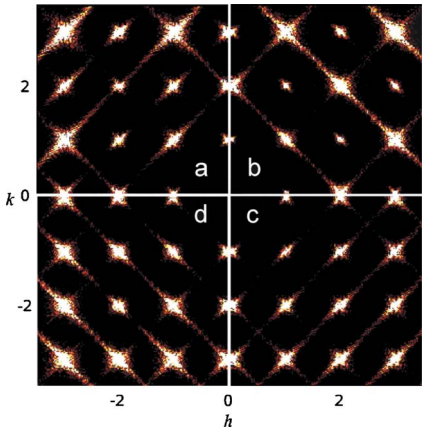

FIG. 7. (Color online) The influence of the magnitudes of ⟨111⟩-directed atomic shifts on the diffuse scattering pattern. 1:1 chemical structure. Each quarter of the (*hk*0) layer is calculated for different sets of displacements. The ratios of $|\boldsymbol{\sigma}_B|/|\boldsymbol{\sigma}_{\mathrm{Pb}}|$ and $|\boldsymbol{\sigma}_{\mathrm{O}}|/|\boldsymbol{\sigma}_{\mathrm{Pb}}|$ are as follows: (a) 1, −1; (b) 1, 0; (c) 0, 0; (d) 0, −1.

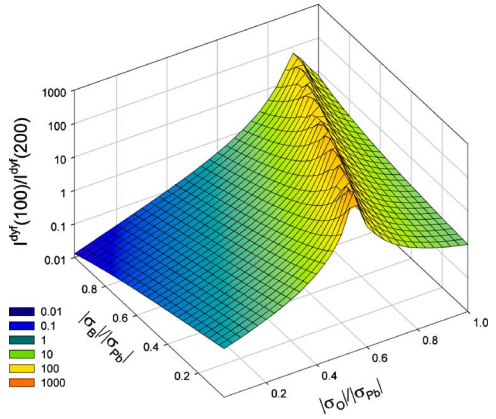

FIG. 8. (Color online) The ratio of diffuse intensities around 100 and 200 reciprocal lattice points calculated for the 1:2 chemical structure with ⟨111⟩-directed atomic shifts as a function of the relative magnitudes of the atomic shifts of B'/B'' and O atoms.

fuse scattering is shown in Fig. 5. It is obvious that the models, which have order-disorder phase transition, have two temperature regions and the higher the temperature, the larger the state change probability on a given site. With respect to this fact, for small values of kT only the most energetically favorable changes are accepted, which gives rise to the ordered state. Here, the situation is significantly different because random field existence causes intrinsic disorder independent of the temperature. This fact, coupled with the well known critical slowing down of the Metropolis algorithm, is the reason that for small kT there are a lot of polar domains in the structure [Fig. 5(b)]. Increasing the temperature would allow for more changes and polar domains are slightly bigger [Fig. 5(a)]. As a consequence, more extended {110}-type planes contribute to sharp and narrow diffuse scattering rods.

As can be seen in Fig. 5, for structures with chemical LRO, the larger the D, the smaller the size of polar domains (boundaries), which gives rise to broadening of the streaks. For a random field strong enough to deform domain walls, a unique (not observed in real samples) diffuse scattering effect appears [Fig. 5(c)]. A similar effect is observed for short-range chemical order, the only change is the shift of "critical" D to lower values. This means that for our models, the main impact of chemical disorder on polar domain structure consists in limiting long-range order and the model does not predict any relationship between polar domain and chemical domain distributions.

The results are qualitatively the same for all directions of displacement (Fig. 6), which is in agreement with the statement that atomic shifts are not important themselves but the relative displacements are. It is worthwhile to emphasize that we give an alternative explanation here for the diffuse scattering origin which is shown in several mentioned papers[25,31,34,48] where the concept of pancakes is developed. In contrast to essentially two-dimensional pancakes, our polar nanodomains are three-dimensional with {110}-oriented domain walls. As stated before, the atoms are not necessarily shifted along ⟨110⟩.

As briefly mentioned in the previous section, generated structures can be modified by applying different magnitudes of cationic shifts. Furthermore, oxygen atoms can also be displaced from their original positions (which is especially important for the interpretation of neutron diffraction patterns) by applying a simple scheme, similar to the one presented by Welberry *et al.*,[31] where the direction of the oxygen shift is opposite to an average vector of displacements of neighboring cations (four Pb and two B'/B''). Such modifications do not affect the general shape of diffuse scattering, although they can alter the intensities for a given reciprocal space area. To illustrate this effect, we present in Fig. 7 four quarters of the (*hk*0) layer obtained for four sets of the shift parameters. The extinction of rods passing through points where $h+k$=odd can be seen in Fig. 7(b), implying that the reason for this is the correlation between shifts of Pb and B'/B'' atoms. The pattern shown in Fig. 7(a) indicates that the shifts of oxygen atoms can suppress the effect of extinction to some extent (it was also observed by Welberry *et al.*[31]).

Hirota *et al.*[24] reported the extinction of diffuse scattering around 200 Bragg reflection observed for PMN. Such observations can give us a hint on the relative values of the atomic shifts. In Fig. 8, we present a map of the ratio of diffuse intensities around 100 and 200 reciprocal lattice points calculated for 1:2 chemical structure with ⟨111⟩-directed atomic shifts as a function of $|\boldsymbol{\sigma}_B|/|\boldsymbol{\sigma}_{\mathrm{Pb}}|$ and $|\boldsymbol{\sigma}_{\mathrm{O}}|/|\boldsymbol{\sigma}_{\mathrm{Pb}}|$. A narrow ridge reaching a value of ~400 indicates an area where the diffuse scattering around 200 practically vanishes. By observing experimentally such characteristic features, one can try to grasp the relations between atomic shifts and to estimate their actual magnitudes.

The final results of the modeling and optimization of the RFE structure (1:2 stoichiometry, chemical SRO) are presented in Fig. 9, where four sections of the reciprocal space and three cuts of the simulated structure generated for ⟨110⟩ directions of atomic displacements are presented. Three perpendicular sections of the crystal clearly show the three-dimensional character of polar domain with domain walls parallel to {110}. The lack of diffuse lines in the (*hk*0.2)

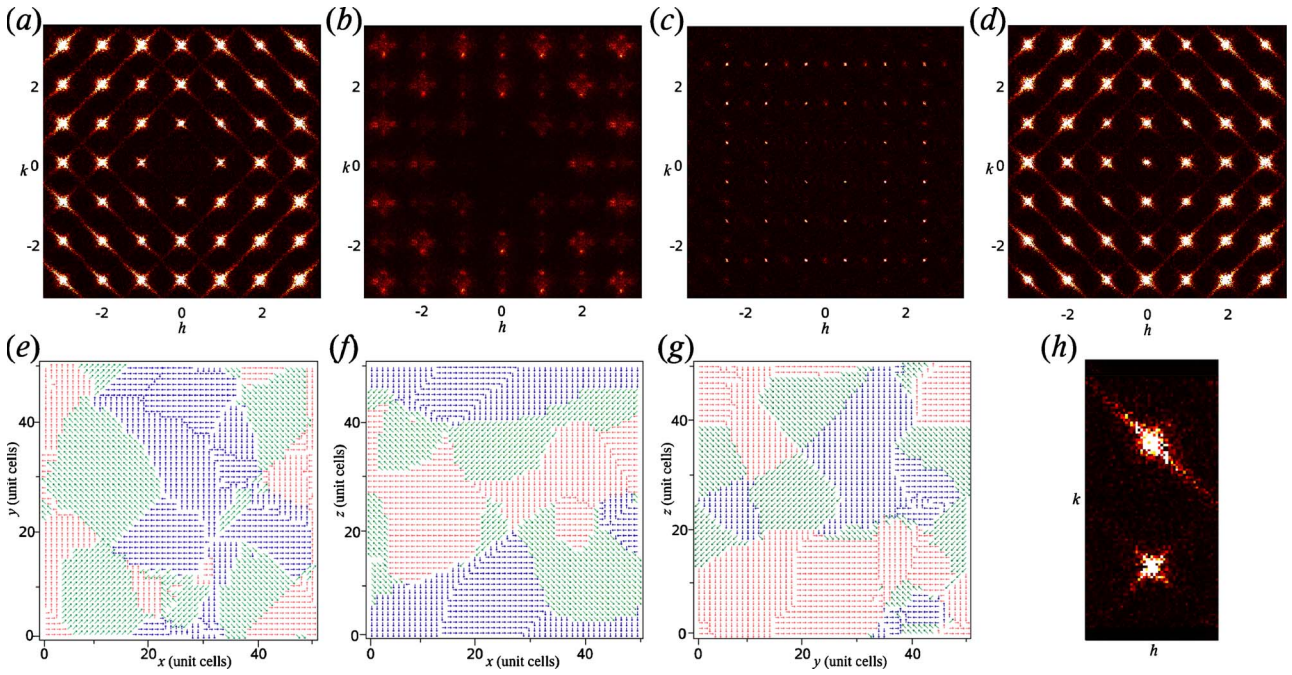

FIG. 9. (Color online) Diffraction effects obtained for the extended model (1:2 chemical structure with SRO, $kT=J$, $D=J$) for four sections of the reciprocal space: (a) ($hk0$), (b) ($hk0.2$), (c) ($hk0.5$), and (d) ($hk1$). Below, three sections of the crystal are shown: (e) xy plane, (f) xz plane, and (g) yz plane. Arrows represent different directions of atomic shifts along ⟨110⟩; colors depict their sense: red is up, blue is down, and green is in the plane of the picture. (h) Details of diffuse scattering around 100 and 110 Bragg reflections.

section indicates the one-dimensional character of the diffuse scattering. Dots around h, k=integer indicate the presence of rods inclined to the ($hk0$) plane and directed along ⟨110⟩ directions lying out of plane. The same can be seen on the ($hk0.5$) section, along with superlattice spots coming from chemical domains. Details of diffuse scattering around 100 and 110 Bragg spots are presented in Fig. 9(h) with characteristic (observed in all experiments) butterfly and elliptic shapes. The crystal configuration presented in Fig. 9 was obtained for ⟨110⟩ shift directions and the following model parameters: $kT=J$, $D=J$. Atomic shifts were optimized to Pb 5%, B'/B'' 1%, and O 2% of the lattice parameter. The final results excellently fit the experimental diffuse scattering data.

IV. CONCLUSIONS

MC modeling and model optimization turned out to be powerful tools enabling an insight into the complex structure of RFE. We have proposed simple models of correlations which take into account two major facts: (i) the tendency of the system to build polar domains and (ii) the chemical disorder impact on the displacement of atoms. The most important achievement of the modeling is the finding that the diffuse scattering does not necessarily come from polar planes and the pancake model does not have to be the actual one. Our results unambiguously indicate the existence of three-dimensional polar nanodomains with {110}-oriented domain walls and ⟨110⟩-directed relative interdomain atomic shifts. It is the only condition necessary to get the diffuse scattering pattern compatible with the experiments; atoms are not necessarily shifted along ⟨110⟩ , and it is not possible to determine the atomic shift directions in RFEs based purely on the analysis of diffuse scattering effects. Our results are in accordance with the microscopical experimental results showing evidence of three-dimensional PNRs. Also, the high intensity diffuse scattering concentrated around Bragg spots suggests the existence of the volume domains.

Proposed models are sensitive to the basic parameters (temperature, random field), which results in different structures obtained from simulations and different respective diffuse scattering patterns enabling the interpretation of the experimental results. However, the intensities of diffuse scattering are sensitive to the relative magnitudes of the atomic displacements. Therefore, when satisfying results are obtained in terms of the shape of diffuse effects, the reverse Monte Carlo procedure with the structure of displacements as a constraint can be applied, enabling further refinement of scattering intensities.

ACKNOWLEDGMENTS

This work was supported by the Polish Ministry of Education and Science from budget funds for science for 2005–2007 as Grant No. 3 T09A 164 28. M.P. would like to thank The Klaus Tschira Foundation (Heidelberg, Germany). The authors would like to thank Stefano Leoni for valuable discussions.

[1] N. Setter and L. E. Cross, J. Appl. Phys. **51**, 4356 (1980).
[2] F. Chu, N. Setter, and A. F. Tagantsev, J. Appl. Phys. **74**, 5129 (1993).
[3] A. I. Agranovskaya, Izv. Akad. Nauk SSSR, Ser. Fiz. **24**, 1275 (1960).
[4] C. G. G. Stenger and A. J. Burggraaf, Phys. Status Solidi A **61**, 275 (1980).
[5] C. A. Randall, S. A. Markgraf, A. S. Bhalla, and K. Baba-Kishi, Phys. Rev. B **40**, 413 (1989).
[6] K. Z. Baba-Kishi and D. J. Barber, J. Appl. Crystallogr. **23**, 43 (1990).
[7] Z. C. Kang, C. Caranoni, I. Siny, G. Nihoul, and C. Boulesteix, J. Solid State Chem. **87**, 308 (1990).
[8] P. Bonneau, P. Garnier, G. Calvarin, E. Husson, J. R. Gavarri, A. W. Hewat, and A. Morell, J. Solid State Chem. **91**, 350 (1991).
[9] N. de Mathan, E. Husson, G. Calvarin, J. R. Gavarri, A. W. Hewat, and A. Morell, J. Phys.: Condens. Matter **3**, 8159 (1991).
[10] C. Caranoni, P. Lampin, I. Siny, J. G. Zheng, Q. Li, Z. C. Kang, and C. Boulesteix, Phys. Status Solidi A **130**, 25 (1992).
[11] C. Caranoni, P. Lampin, and C. Boulesteix, Powder Diffr. **8**, 191 (1993).
[12] K. S. Knight and K. Z. Baba-Kishi, Ferroelectrics **173**, 341 (1995).
[13] K. Z. Baba-Kishi, G. Cressey, and J. Cernik, J. Appl. Crystallogr. **25**, 477 (1992).
[14] K. Z. Baba-Kishi, P. M. Woodward, and K. Knight, Ferroelectrics **261**, 21 (2001).
[15] C. Malibert, B. Dkhil, J. M. Kiat, D. Durand, J. F. Berar, and A. Spasojevic-de Bire, J. Phys.: Condens. Matter **9**, 7485 (1997).
[16] W. Dmowski, M. K. Akbas, P. K. Davies, and T. J. Egami, J. Phys. Chem. Solids **61**, 229 (2000).
[17] P. M. Woodward and K. Z. Baba-Kishi, J. Appl. Crystallogr. **35**, 233 (2002).
[18] M. P. Harmer, A. S. Bhalla, and B. Fox, Mater. Lett. **2**, 278 (1984).
[19] H. M. Chan, M. P. Harmer, and A. S. Bhalla, Jpn. J. Appl. Phys., Suppl. **24**, 550 (1985).
[20] C. Boulesteix, F. Varnier, A. Llebaria, and E. Husson, J. Solid State Chem. **180**, 141 (1994).
[21] L. A. Bursill, J. L. Peng, H. Qian, and N. Setter, Physica B **205**, 305 (1995).
[22] L. A. Bursill, Ferroelectrics **191**, 129 (1997).
[23] M. Yoshida, S. Mori, N. Yamamoto, Y. Uesu, and J. M. Kiat, Ferroelectrics **217**, 327 (1998).
[24] K. Hirota, Z.-G. Ye, S. Wakimoto, P. M. Gehring, and G. Shirane, Phys. Rev. B **65**, 104105 (2002).
[25] G. Xu, Z. Zhong, H. Hiraka, and G. Shirane, Phys. Rev. B **70**, 174109 (2004).
[26] T. R. Welberry, *Diffuse X-Ray Scattering and Models of Disorder* (Oxford University Press, Oxford, 2004).
[27] H. You and Q. M. Zhang, Phys. Rev. Lett. **79**, 3950 (1997).
[28] B. Chaabane, J. Kreisel, B. Dkhil, P. Bouvier, and M. Mezouar, Phys. Rev. Lett. **90**, 257601 (2003).
[29] N. Takesue, Y. Fujii, and Hoydoo You, Phys. Rev. B **64**, 184112 (2001).
[30] H. Hiraka, S.-H. Lee, P. M. Gehring, G. Xu, and G. Shirane, Phys. Rev. B **70**, 184105 (2004).
[31] T. R. Welberry, M. J. Gutmann, Hyungje Woo, D. J. Goossens, Guangyong Xu, C. Stock, W. Chen, and Z.-G. Ye, J. Appl. Crystallogr. **38**, 636 (2005).
[32] S. Vakhrushev, A. Ivanov, and J. Kulda, Phys. Chem. Chem. Phys. **7**, 2340 (2005).
[33] G. Xu, G. Shirane, J. R. D. Copley, and P. M. Gehring, Phys. Rev. B **69**, 064112 (2004).
[34] G. Xu, Z. Zhong, Y. Bing, Z.-G. Ye, and G. Shirane, Nat. Mater. **5**, 134 (2006).
[35] C. Stock, D. Ellis, I. P. Swainson, Guangyong Xu, H. Hiraka, Z. Zhong, H. Luo, X. Zhao, D. Viehland, R. J. Birgeneau, and G. Shirane, Phys. Rev. B **73**, 064107 (2006).
[36] B. P. Burton, E. Cockayne, and U. V. Waghmare, Phys. Rev. B **72**, 064113 (2005).
[37] B. I. Halperin and C. M. Varma, Phys. Rev. B **14**, 4030 (1976).
[38] H. Qian and L. A. Bursill, Int. J. Mod. Phys. B **10**, 2027 (1996).
[39] R. Fisch, Phys. Rev. B **67**, 094110 (2003).
[40] B. P. Burton, E. Cockayne, S. Tinte, and U. V. Waghmare, Phase Transitions **79**, 91 (2006).
[41] S. Tinte, B. P. Burton, E. Cockayne, and U. V. Waghmare, Phys. Rev. Lett. **97**, 137601 (2006).
[42] U. V. Waghmare, E. J. Cockayne, and B. P. Burton, Ferroelectrics **291**, 187 (2003).
[43] A. Pietraszko, B. Hilczer, and C. Caranoni, Ferroelectrics **298**, 235 (2004).
[44] M. Paściak, M. Wołcyrz, and A. Pietraszko, Acta Crystallogr., Sect. A: Found. Crystallogr. **A62**, s195 (2006).
[45] H. Qian, J. L. Peng, and L. A. Bursill, Int. J. Mod. Phys. B **7**, 4353 (1993).
[46] N. Metropolis, A. W. Rosenbluth, M. N. Rosenbluth, A. H. Teller, and E. Teller, J. Chem. Phys. **21**, 1087 (1953).
[47] M. A. Akbas and P. Davies, J. Am. Ceram. Soc. **83**, 119 (2000).
[48] Guangyong Xu, P. M. Gehring, and G. Shirane, Phys. Rev. B **74**, 104110 (2006).
[49] B. Dkhil, J. M. Kiat, G. Calvarin, G. Baldinozzi, S. B. Vakhrushev, and E. Suard, Phys. Rev. B **65**, 024104 (2001).
[50] R. Haumont, B. Dkhil, J. M. Kiat, A. Al-Barakaty, H. Dammak, and L. Bellaiche, Phys. Rev. B **68**, 014114 (2003).
[51] A. I. Frenkel, D. M. Pease, J. Giniewicz, E. A. Stern, D. L. Brewe, M. Daniel, and J. Budnick, Phys. Rev. B **70**, 014106 (2004).
[52] T. Proffen and R. B. Neder, J. Appl. Crystallogr. **30**, 171 (1997).
[53] R. Potts, Proc. Cambridge Philos. Soc. **48**, 106 (1952).
[54] A. Guinier, *X-ray Diffraction in Crystals, Imperfect Crystals and Amorphous Bodies* (Freeman, San Francisco, 1963).
[55] M. A. Krivoglaz, *Theory of X-ray and Thermal-Neutron Scattering by Real Crystals* (Plenum, New York, 1969).
[56] V. Gosula, A. Tkachuk, K. Chung, and H. Chen, J. Phys. Chem. Solids **61**, 221 (2000).
[57] A. Tkachuk and H. Chen, AIP Conf. Proc. **677**, 55 (2003).